Modeling the Simultaneous Two Ground-State Lasing Emissions in Chirped Quantum Dot Lasers

Gray Lin, Van-Truong Dai, and Chien-Ping Lee
Dept. of Electronics Engineering, National Chiao-Tung Univ., Hsinchu, 30010, Taiwan, R.O.C.

***Abstract*-Rate-equation model is employed to investigate the anomalous threshold lasing spectra of chirped quantum dot lasers. Simultaneous two-wavelength lasing is attributed to two ground-state emissions from chirped multilayers of InAs/InGaAs quantum dots.**

I. INTRODUCTION

Self-assembled quantum dots (QDs) are subjected to inhomogeneity in shapes, sizes, as well as compositional non-uniformity. Optical emitters incorporated with QD gain media are therefore characterized with low saturated gain but broad gain spectra. Moreover, QD lasers with multilayer stacking, either uniform or chirped [1, 2], exhibit device characteristics and spectral behaviors very different from conventional quantum well lasers.

Simultaneous ground-state (GS) and excited-state (ES) lasing emissions well above threshold were demonstrated for uniform-stacked 3-layer QD lasers in [2]. Master-equation model was employed to explain these results. Incomplete gain clamping and retarded carrier relaxation is identified as the origin of that effect.

In this paper, rate-equation model is carried out to theoretically analyze our recent experimental works of simultaneous two-wavelength lasing emissions around threshold in chirp multilayer QD lasers [1]. Inter-well transport in multilayer QD structure as well as linear optical gain for chirped QD ensembles is included to consistently explain the measured results.

II. THEORETICAL MODEL

The light-current-spectrum characteristics of QD lasers can be theoretically calculated by solving a coupled set of carrier and photon rate equations [3, 4], taking into account both the size distribution of QDs and a series of longitudinal cavity modes.

Each QD is assumed to have discrete GS and ES, as well as continuum-like upper states (US), with degeneracy of 2, 6, and 30, respectively. Condition of charge neutrality is assumed and an electron-hole pair is treated as an exciton. Relaxation and recombination can occur only within the same QDs and approximated by a common time constant [4].

InAs wetting layer and InGaAs QW layer, where InAs QDs are embedded, serve as carrier reservoirs for QDs and are modeled by one discrete level with degeneracy of 100. Since carrier populations among multilayer QDs is facilitated only through QW states, carrier distribution among multilayer structure is better described by transport between neighbor wells. For simplicity, we assume that all carriers are injected into the QW state in the first layer. An inter-well transport time is adopted for the first time to access the non-uniform contribution intrinsic in chirped multilayer QD structure.

Based on the density-matrix equation as suggested in [4], linear optical gain for each group of QD ensembles contributing to multi-longitudinal photon modes is separately calculated for subsequent convolution integral. Homogeneous broadening due to polarization dephasing is considered by Lorentzian lineshape function while inhomogeneous broadening due to the dot size fluctuation is represented by Gaussian distribution function.

III. RESULTS AND DISCUSSION

The calculation model shown above is applied first to the uniform 3-layer QD lasers as in [2] and then to the chirped 10-layer QD lasers shown in Fig. 1. Chirped multilayer QD layers with 2-, 3- and 5-layer of longer-, medium- and short-wavelength QD stacks (designated as $2*QD_L$, $3*QD_M$ and $5*QD_S$) are engineered in the laser structure, which corresponding to InAs QDs of 2.6 ML capped by InGaAs of 4 nm, 3 nm and 1 nm, respectively. The stacking sequence is arranged so that QD_L is near the n-side.

The carrier relaxation time in QDs (i.e. $\tau_{ue}=\tau_{eg}=\tau_{ug}$) is taken as 7 ps while the radiative recombination time (τ_r) is taken as 0.75 ns, without any dependence on QD states to a first approximation. However, the carrier relaxation time constants from QW states to US of QDs (i.e. τ_{wu}) are setting parameters dependent on energy separation of ΔE_{wu}. The relation between relaxation and escape times is dictated by the principle of detailed balance.

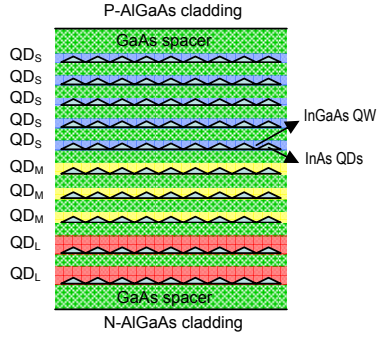

Figure 1. The schematic diagram of chirped multilayer QD structure.

This work was supported by the Ministry of Education under the Aiming for the Top University and Elite Research Center Development Plan, Taiwan National Science and Technology Program for Nanoscience and Nanotechnology (NSC 97-2120-M-009-004) and the National Science Council (NSC 97-2221-E-009-158).

In uniform 3-layer QD lasers, consistent calculated emission spectra of simultaneous GS and ES lasing well above threshold are achieved both with and without inter-well transport. The only difference is the carrier populations in the QW and QD states are higher in the first layer. An inter-well transport time of 0.1 ps shows almost even carrier distribution, which is the case in MQW system with large conduction band offset [5]. Uniform multilayer structure can therefore be lumped into one group without transport.

For chirped 10-layer QD lasers, $2*QD_L$, $3*QD_M$ and $5*QD_S$ are lumped into three groups with inter-group transport time of 0.5 ps. The center wavelengths of QD_L, QD_M and QD_S are experimentally determined to be 1261 nm, 1220 nm and 1170 nm, respectively, for the GS and 1183 nm, 1146 nm and 1102 nm, respectively, for the ES. Other parameters we used are as follows. The QD density per layer is $5*10^{10}$ cm^{-2}. The full width at half maximum (FWHM) of inhomogeneous and homogeneous broadening are 25 meV and 15 meV, respectively. The cavity length is 2 mm, the optical confinement factor per layer is 0.0075, as-cleaved mirror reflectivity is 32%, the cavity loss is 4.7 cm^{-2}, the effective refractive index is 3.5, and the stripe width is 5 μm.

The calculated light-emission spectra are shown in Fig. 2. Simultaneous two-wavelength lasing around threshold current of 30 mA is well resolved from two GS of QD_L and QD_M with peak wavelength of 1261 nm and 1215 nm, respectively. Fig. 3 shows the average populations as a function of injection current for individual GS and ES of QD_L, QD_M and QD_S. The origin of the effect is attributed to the carrier population of $3*QD_M^{GS}$ is pinned at threshold gain approximately of the same level as the saturated gain of $2*QD_L^{GS}$. That the QD_L^{ES} population increases at a higher rate than QD_M^{ES} and QD_S^{GS} is due to the lower energy state of QD_L^{ES}. By the way, saturated population of QD_S^{GS} and increasing higher population of QD_S^{ES} do not contribute to emission spectra as they are subjected to large absorption. Note that carrier leakage under high current injection may be severe and is not considered in our calculation. Fig. 4 shows the percentage of carrier recombination in all QD states and QW state. Most of injected current recombines through QD states. Below lasing threshold, carrier distribution per-QD layer is higher in longer-wavelength QD-stack near the n-side. However, carrier pinning and retarded relaxation render decreasing fraction of current recombination above threshold.

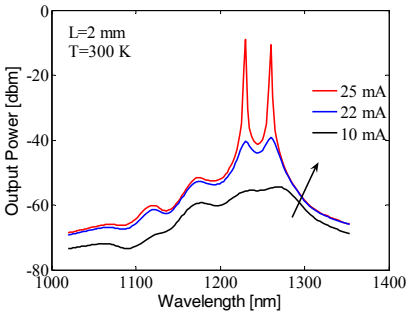

Figure 2. The light-emission spectra of chirped multilayer QD lasers.

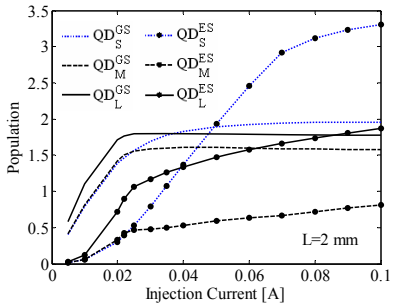

Figure 3. The average populations of QD states versus injection current.

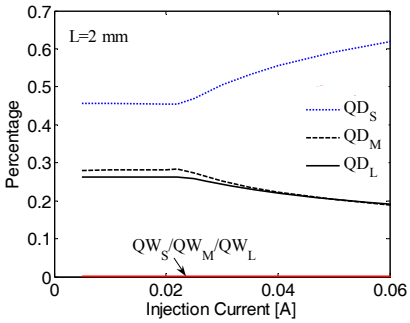

Figure 4. The percentage of carrier recombination versus injection current in chirped multilayer structure.

IV. Summary

We have theoretically analyzed the chirped 10-layer QD lasers. The average population of QD states and the percentage of recombined carriers among chirped multilayers are quantitatively understood within a rate-equation model. Simultaneous two GS lasing emissions around threshold is attributed to the threshold gain of medium-wavelength QD-stack is pinned to the saturated gain of longer-wavelength QD-stack at the particular cavity length. A further understanding of the lasing properties of various QD material systems may lead to improved device performance as well as novel device applications.

References

[1] G. Lin et al., "Novel chirped multilayer quantum dot laser," *Proc. SPIE*, Vol. 6997, pp. 69970R, April 2008.

[2] A. Markus et al., "Simultaneous two-state lasing in quantum-dot lasers," *Appl. Phys. Lett.*, vol. 82, pp. 1818-1820, March 2003.

[3] C. Meuer et al., "Static gain saturation in quantum dot semiconductor optical amplifiers," *Opt. Exp.*, Vol.16, pp. 8269-8279, May 2008.

[4] M. Sugawara, K. Mukai, Y. Nakata, and H. Ishikawa, "Effect of homogeneous broadening of optical gain on lasing spectra in self-assembled $In_xGa_{1-x}As/GaAs$ quantum dot lasers," *Phys. Rev. B*, vol. 61, pp. 7595-7603, 2000.

[5] A. Hangleiter, A. Grabmaier, and G. Fuchs, "Damping of the relaxation resonace in multiple-quantum-well lasers by slow interwell transport," *Appl. Phys. Lett* , vol. 62, pp. 2316-2318, May 1993.

Non-ideal quantum dots (QDs) formed by self-assembled growth are subjected to inhomogeneity in shapes, sizes, and compositions, which results in rather broad gain spectra but lower saturated optical gain if incorporated as the active media in diode lasers.

Experimental characterization of unique device properties as well as theoretical analysis of anomalous spectral behaviors will certainly provide important guidelines for further optimization and future applications.

The rate equations employed are similar to those used in [3].

[4] M. Sugawara et al., "Theory of optical signal amplification and processing by quantum dot semiconductor optical amplifiers," *Phys. Rev. B*, vol. 69, pp. 235332, 2004.

[5] J. L. Xiao and Y. Z. Huang, "Numerical analysis of gain saturation, noise figure, and carrier distribution for quantum-dot semiconductor-optical amplifiers", *IEEE J. Quantum Electron.*, Vol. 44, No. 5, pp. 448-455, May 2008.